Simplified Modeling of Non-Ideal Blast Waves from Metallized Heterogeneous Explosives

Zouya Zarei[1], David L. Frost[1], Laura Donahue[2], and David R. Whitehouse[2]
[1]McGill University, Mechanical Engineering Department, Montreal, Quebec, Canada
[2]Martec Ltd., Halifax, Nova Scotia, Canada

Corresponding author, D. L. Frost: david.frost@mcgill.ca

Introduction

Most commercial and military explosives are oxygen deficient. As a result, after the detonation of a high explosive charge, a significant amount of energy release can occur as the hot detonation products expand, mix, and react with the surrounding air. Afterburning has been extensively studied for confined explosions, where shock reverberations and turbulent mixing augment the burning within the combustion products (e.g., Kuhl et al. 2003). The present paper is concerned rather with the effect of afterburning on the blast wave generated from *unconfined* explosives. Of particular interest is the effect of afterburning from explosives that contain a large mass fraction of reactive metal powders. For so-called metalized explosives, the afterburning is due to the oxidation of the added metal particles as well as the unreacted detonation product species. The particles may burn primarily in the combustion products or the surrounding atmosphere, depending on the particle size. Very fine particles will react rapidly, but as the expanding combustion products decelerate, drag will limit the extent of particle dispersal and the particles will burn largely within the hot combustion products gases or near the combustion product interface. Larger particles will be dispersed to a greater distance and will burn in the shocked air behind the blast wave or may overtake the blast wave front and possibly burn in the surrounding quiescent air. The coupling between the energy release from the metal particle reaction and the dynamics of the blast wave will depend on the spatial and temporal variation of the afterburning energy release. In the present paper, the detailed multiphase dynamics that occur when a metalized explosive is detonated are not considered. Rather, this coupling mechanism is explored by introducing the afterburn energy in a simplified manner in a single phase model for the explosion process.

For unconfined afterburning explosives the properties of the blast wave generated (e.g., peak pressure and impulse) will depend on the fraction of the total energy release that occurs as afterburning, the rate of afterburning, as well as the spatial region over which the energy is deposited and will not, in general, scale with the overall energy released. Various approaches have been taken to model the blast wave generated from non-ideal afterburning explosives in which the energy release occurs over a time comparable to that for the expansion of the fireball. Detailed multiphase reactive-flow modeling of the process is computationally intensive (e.g., Needham 2004) and requires the specification of constitutive physical models for particle-particle interactions, particle drag and the particle reaction mechanisms with various oxidizers. However, many of these physical processes are poorly understood under the high-speed flow conditions that occur during fireball expansion. Other, more simplified models do not consider the detailed near-field reactive fluid flow. For example, one approach is to consider the expansion of the combustion products as a spherical piston (e.g., Taylor 1946, Dewey 1971).

1

Specification of a given piston motion will then generate a particular flow field, although the piston motion is not connected directly with the energy release profile. A second simplified approach is to use a compressible-flow model to track the propagation of a shock wave generated by the bursting of a high-pressure sphere. Ritzel and Matthews (1997) and later Donahue et al. (2004) used this "balloon analogue" approach, based on the bursting-sphere blast wave solution of Brode (1959), in which the initial balloon properties (size, gas pressure, temperature, gamma, and molecular weight) can be chosen to match a given blast wave profile. Although the near-field blast wave behaviour is not realistic for this model, they obtained good results in matching blast wave profiles in the mid- and far-field. Ritzel and Matthews (1997) used their model to simulate the effect of afterburning on blast wave propagation. They assumed that some fraction of the energy release was expended over a characteristic time corresponding to the reaction of incompletely reacted fuel which produced additional gaseous products within the explosion products. In the present investigation, the earlier work by Ritzel and Matthews (1997) and Donahue et al. (2004) has been extended to include the effect of afterburning due to the energy release from the formation of condensed metal oxides, which does not produce additional gaseous products. In addition, the effect of the spatial location of the energy release on the blast wave dynamics has been investigated.

Results

Martec Ltd.'s IFSAS-II compressible-flow CFD code (Donahue et al., 2004) was used to investigate various afterburning scenarios following the burst of a high-pressure sphere in which the initial conditions correspond to the energy release from a 1 kg charge of TNT. To investigate the effect of the spatial variation of the afterburning energy release, two limiting cases were considered, and compared with the case of no afterburn: i) release of the afterburn energy (including the possibility of the generation of additional gaseous species) uniformly within the combustion products (to simulate the reaction of fine metallic particles), and ii) release of the afterburn energy directly behind the blast wave (to simulate the case in which the burning particles form a layer that follows closely behind the blast wave). In reality, the dispersed burning particles will form a cloud with a density distribution varying in time and space, with the complex dynamics of the cloud motion dependent on the particle size, density, and fluid properties. The multiphase flow produced by explosively dispersed particles has been considered by previous researchers (e.g., Lanovets et al., 1991; Zhang et al., 2001) and is beyond the scope of the present paper.

In summary, the four particular cases that were considered are as follows: i) immediate release of all the energy by the bursting of the sphere (i.e., no afterburn), ii) immediate release of 50% of the energy followed by the release of the remainder of the energy as afterburn resulting in the formation of gaseous products within the explosion products fireball, iii) a similar energy partition as in case ii), but with the afterburn energy released as internal energy due to the oxidation of metal particles within the fireball, and iv) 50% of the total energy released as afterburn, but released in a zone immediately behind the blast wave. For the case of afterburning within the fireball, the afterburn energy was released over a period of 1.86 ms, which corresponds to the time for the fireball radius to reach about 75% of the maximum diameter. For case iv), the energy was released 10 times faster to ensure that the energy release occurred over a very narrow region behind the shock.

2

Following the detonation of a spherical metalized explosive charge, as the particles move radially outwards, the overall number density of the dispersed particle cloud follows an inverse square relationship with respect to the distance from the charge. Since the amount of energy released by the combustion of particles is proportional to the number density of the particles in the combustion zone, the energy release profile for case iv) was thus set to satisfy

$$E_{AB}(r) = C\left[\frac{1}{r^2} + b\right]$$

The two constants are determined by specifying the total afterburn energy and the range over which it occurs.

Figure 1 shows the shock wave pressure traces at a distance of 2 m from the charge for the cases i) – iii) described above. With some of the energy released as afterburn, the peak pressure is reduced and the secondary shock moves forward (as found earlier by Ritzel and Matthews, 1997). There is a small difference in the blast wave traces for cases ii) and iii), i.e., with the formation of additional gaseous products (case ii), the blast wave pressure and impulse are slightly higher, but the secondary wave is slightly retarded in time. However, when the energy release follows the shock closely, the blast wave pressure and impulse (shown in Fig. 2 again at a distance of 2 m) are augmented, in comparison with the case i) where all of the energy is released instantaneously.
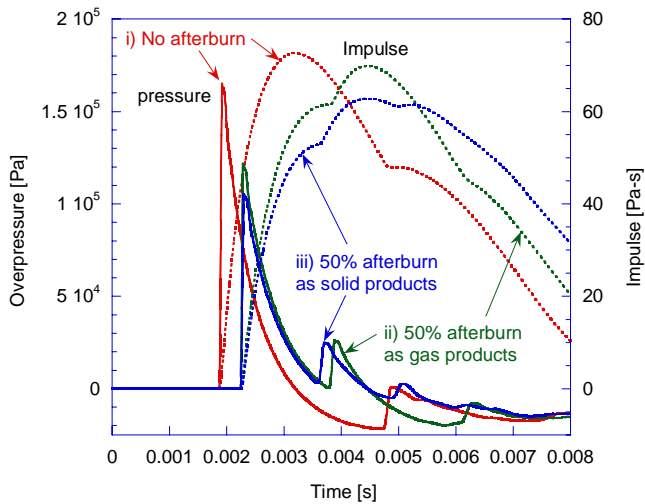

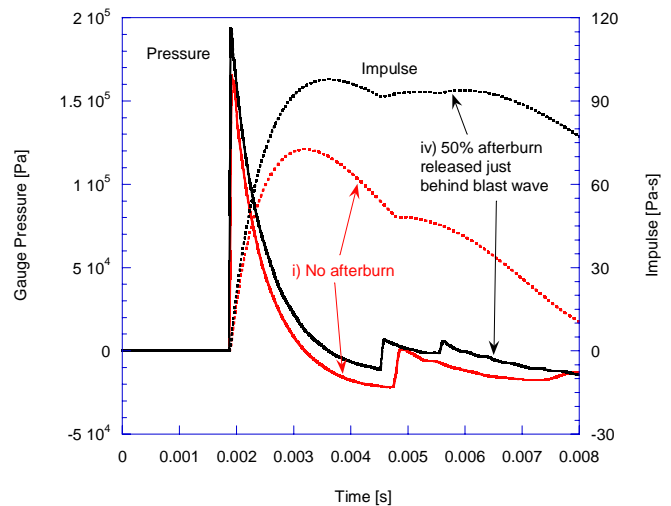Fig. 1 Effect of afterburning on the blast wave pressure and impulse at a distance of 2 m from the charge.

Fig. 2 Blast wave pressure and impulse at a distance of 2 m from the charge for the case of afterburning occurring immediately behind blast wave.
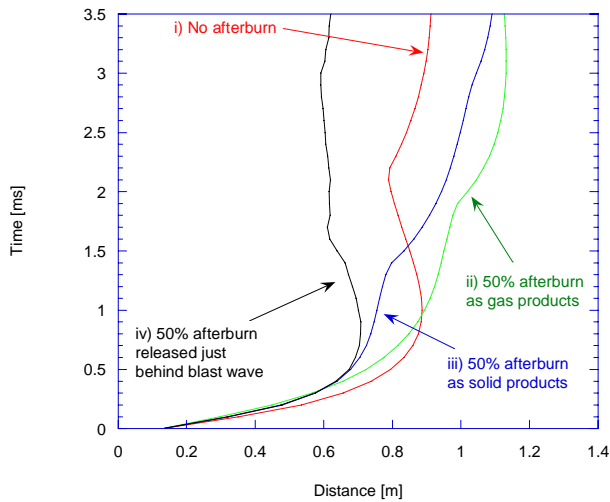
3

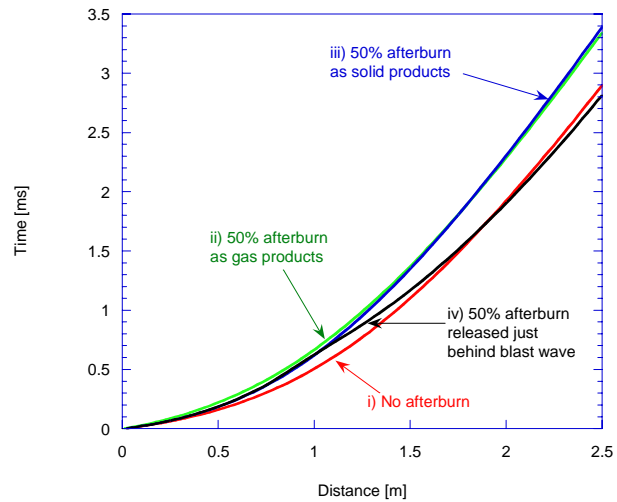Fig. 3 Effect of afterburning on the motion of the combustion products interface position.

Fig. 4 Effect of afterburning on the trajectory of the blast wave.

The location at which the energy is released has a strong influence on the motion of the combustion products interface as well as the blast wave. Figures 3 and 4 show the combustion products interface and blast wave trajectories, respectively, for the four cases considered. When the afterburn energy is deposited within the combustion products, the deceleration of the interface is reduced and the final diameter of the combustion products is increased. When energy is deposited directly behind the blast wave (case iv), the final diameter of the combustion products is about one-half that of the no afterburn case. However, when the energy release closely follows the shock, although initially the blast wave decelerates, after less than one millisecond, the blast wave accelerates due to the energy release. This is in contrast with cases ii) and iii) in which the blast wave is always decelerating. The acceleration occurs over the energy release zone, and leads to a stronger blast wave in the far field compared to case i).

In the case of energy release behind the shock, the initial location of energy release as well as the range over which it is released affect the blast wave propagation. Figures 5 and 6 show the effect of the initial location of energy release on the blast wave, where the distance over which energy is released is kept constant at 1.5m. The energy release was first initiated when the blast wave reached a distance of either 0.5 m or 1 m from the blast centre. Since the energy release profile is $O(1/r^2)$, the highest energy release occurs in the early part of the range over which the afterburning occurs. If the afterburn energy is released near to the charge centre (e.g., at 0.5 m), then although the blast wave motion is accelerated at that point, the acceleration is not sufficient to overcome the initial reduction in the velocity of the blast wave due to the reduced fraction of the energy that is released instantaneously. When the energy release occurs further from the blast center (i.e., the 1 m case shown in Figs. 5 and 6), there is a larger increase in the maximum overpressure and the impulse. In the far field, this increase is sufficient to result in a stronger blast wave than for the case when all of the energy is released instantaneously.

Figures 7 and 8 show the effect of varying the range over which the energy is released while keeping the initial location of energy release constant. Both the energy depositions were initiated at a distance of 1m, with one occurring over 0.5m and the other over 1.5m. The resulting blast wave shows an increased augmentation when the afterburn energy is released over an extended radial distance.
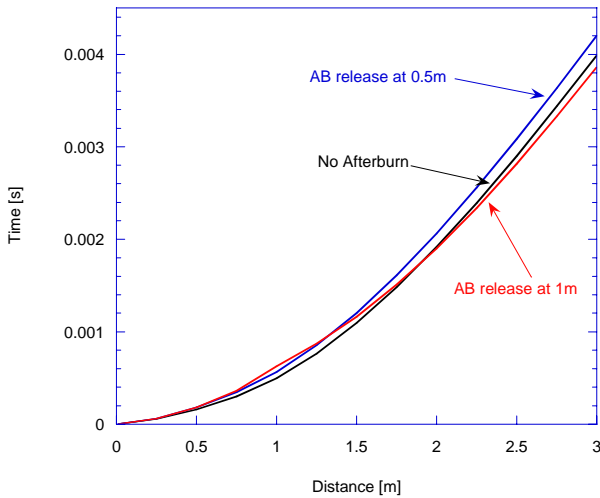

Fig. 5 Effect of the initial location of energy release on the blast wave trajectory for the case of afterburning occurring immediately behind the shock.
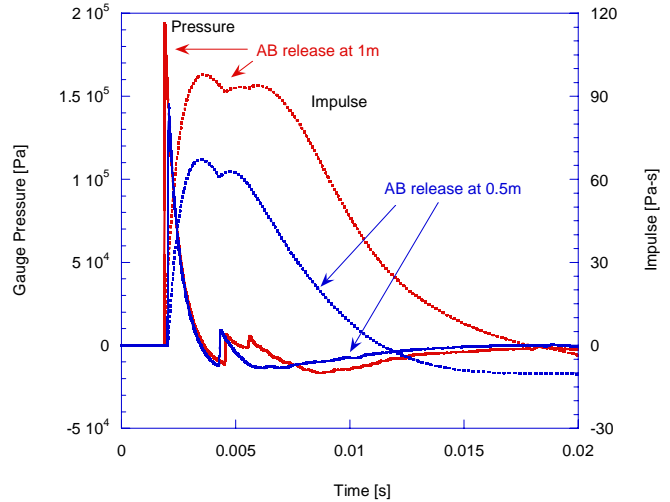
Fig. 6 Effect of the initial location of energy release on the blast wave pressure and impulse at a distance of 2 m from the charge.

Varying the energy deposition rate behind the shock wave had little effect on the resulting blast wave trajectory in the far field. Taking the case of energy release initiated at 1m and occurring over a distance of 1.5m, the rate of energy release was set at a half and a fifth of the release rate used in the other cases involving energy release immediately behind the shock. A small difference was seen in the initial acceleration of the shock near the beginning of the energy release zone (with faster energy release rates resulting in slightly higher accelerations), but the trajectories eventually converge to that depicted in figures 5 and 7. There was also a small reduction in the impulse at 2m when the release rate was slower.
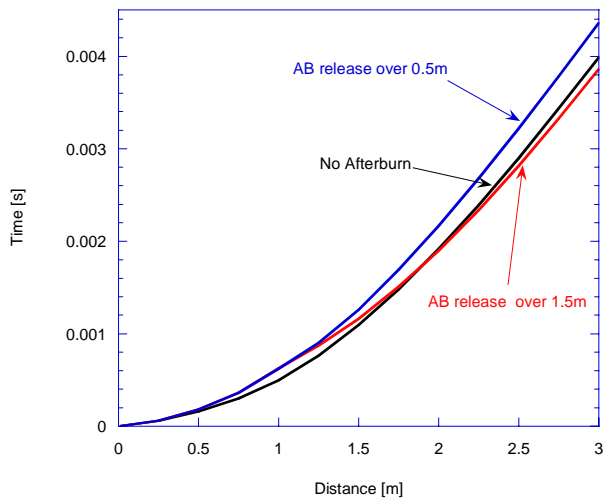
Fig. 7 Effect of the size of the energy release zone on the blast wave trajectory for the case of afterburning occurring immediately behind the shock.
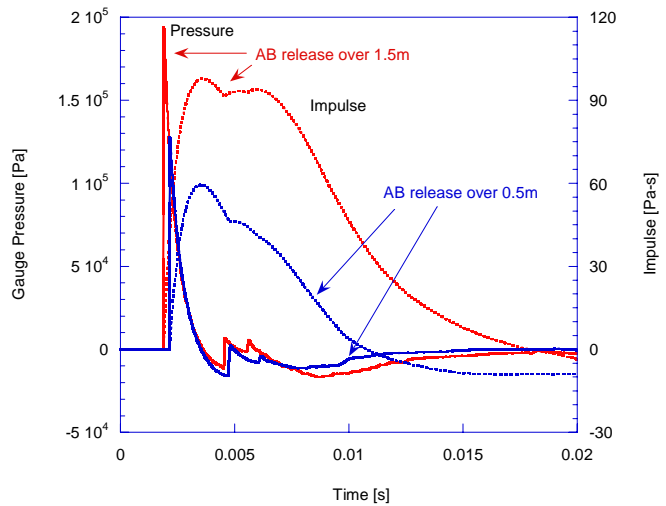
Fig. 8 Effect of the size of the energy release zone on the blast wave pressure and impulse at a distance of 2 m from the charge.

Conclusions

This study investigated the effect of varying the location and release rate of energy as afterburning on the propagation of a blast wave. The case of instantaneous energy release was compared with that of 50% of energy released as afterburn at different locations and release rates. The results indicate that if afterburn energy release occurs within the expanding detonation products, the resulting blast wave and impulse are reduced, particularly in the case of the afterburning of metal particles. There is a higher potential of blast wave augmentation if the energy is released behind the shock wave, which would occur in a scenario in which the metal particles catch up to the primary shock but do not penetrate it. Higher energy release rates (which translate into energy being released in a very narrow zone behind the shock) tend to result in a slightly higher overpressure and maximum impulse. It was also found that with an energy release profile that follows a general inverse square relationship, energy release had to occur further from the blast center and over a more extended range in order to result in a stronger blast wave and a higher impulse than in the case of instantaneous energy release. For a given fraction of the total energy released as afterburn, it is likely that a particular spatial variation in energy release will lead to maximum augmentation of the blast wave strength. Current research is investigating the existence of scaling relationships for the properties of non-ideal blast waves generated by the detonation of afterburning explosives based on a minimum number of parameters.

References

HL Brode 1959 "Blast Wave from a Spherical Charge" *Phys Fluids* 2:217-229.

JM Dewey 1971 "The Properties of a Blast Wave obtained from an Analysis of the Particle Trajectories" *Proc Roy Soc Lond A* 324:275-299.

L Donahue, DR Whitehouse, T Josey, DV Ritzel, and P Winter 2004 "Non-Ideal Blast Effects for Vulnerability/Lethality Analysis" *Proc 18th MABS*, Bad Reichenhall, Germany.

AL Kuhl, RE Ferguson, and JB Bell 2003 "Thermo-Gas-Dynamic Model of Afterburning in Explosions" *Proc. 19th Int. Coll. Dyn. of Expl. And Reactive Sys.*, Hakone, Japan.

VS Lanovets, VA Levich, NK Rogov, Yu-V Tunik, NK Shamshev 1991 "Dispersion of the Detonation Products of a Condensed Explosive with Solid Inclusions," *Fizika Goreniya i Vzryva* 29:88-92.

C Needham 2004 "The ARA High Explosive Afterburn Model" *Proc 18th MABS*, Bad Reichenhall, Germany.

DV Ritzel and K Matthews 1997 "An Adjustable Explosion-Source Model for CFD Blast Calculations" *Proc 21st Int Symp on Shock Waves*, Great Keppel Island, Australia, paper 6590.

GI Taylor 1946 "The Air Wave Surrounding an Expanding Sphere" *Proc Roy Soc Lond A* 186:981-985.

F Zhang, DL Frost, PA Thibault, and SB Murray, 2001 "Explosive Dispersal of Solid Particles," *Shock Waves*, 10:431-443.